ULTRASONIC INSPECTABILITY MODELS FOR JET ENGINE FORGINGS

T. A. Gray

Center for Nondestructive Evaluation
Iowa State University
Ames, IA 50011

INTRODUCTION

Ultrasonic inspections of axially symmetric forgings, such as those used in the manufacture of jet engine rotating components, are typically performed on so-called "sonic shapes" which have relatively simple geometries. Formation of these sonic shapes typically requires an additional machining step, so significant cost savings can result if the inspections can be reliably performed on forgings whose shapes more closely resemble those of the final machined components. However, compound curvatures of the component surface will cause complicated focusing of the ultrasonic beam within the part which will change the inspection sensitivity to flaws of interest. Analytical models of ultrasonic inspection in complex shaped parts can be used to predict the new sensitivity.

This paper demonstrates the application of ultrasonic measurement models to the prediction of ultrasonic inspectability and to the specification of ultrasonic inspection parameters for axially symmetric forgings. Forging geometries are obtained from CAD models. Internal defects are assumed to be either planar or volumetric scatterers whose orientations can be aligned with forging flow lines. Potentially, the flow lines can be obtained from microphotographs or via computer calculations using commercial forging software. The models allow the use of planar or focused ultrasonic transducers that can be oriented either normal to or at oblique incidence to the forging surface. Both longitudinal and shear wave modes can be modeled. Scan line spacing can be varied to analyze the tradeoffs between scan speed and internal ultrasonic coverage of the forging. At present, the computed inspectability parameter is either the raw signal amplitude or distance-amplitude compensated gain. Graphical output of the model shows the inspectability parameter rendered in false color or greyscale and superimposed on the forging profile. Examples of the use of the model will be demonstrated on forgings currently being studied in the Engine Titanium Consortium.

MODEL IMPLEMENTATION

The UT measurement model is based upon Auld's electromechanical reciprocity relationship [1]. Flaws are assumed to occur within the bulk of an isotropic, homogeneous, elastic medium. It is further assumed that the flaw dimensions are small with respect to the ultrasonic beam size and that their scattering amplitudes do not vary significantly over the range of angles subtended by the transducer. The ultrasonic inspection method is assumed

Review of Progress in Quantitative Nondestructive Evaluation, Vol. 17
Edited by D.O. Thompson and D.E. Chimenti,, Plenum Press, New York, 1998

to be pulse-echo. This results in a relatively simple ultrasonic measurement model in which the ultrasonic beam propagation effects and the scattering effects are separable [2]. This model predicts the time harmonic (single frequency) response caused by the presence of a scatterer in the ultrasonic beam.

Ultrasonic beam propagation and transmission and/or refraction through curved liquid-solid interfaces are represented by the Gaussian-Hermite beam model, in which a time harmonic ultrasonic displacement or velocity field is represented as a summation of Gaussian-Hermite functions [3]. This model employs paraxial approximations, whose accuracy is best near the beam axis and for cases where incident angles in the beam footprint on the component surface are not near critical angles. This model is used to predict bulk propagating waves only. Scattering amplitudes for circular flat-bottomed holes are modeled using the elastodynamic Kirchhoff approximation [4]. This model accurately predicts the specular reflection from planar and volumetric reflectors, but does not correctly predict edge diffraction, internal reverberations, or surface waves on the reflector.

The time harmonic result just described must be convolved with the system response of an ultrasonic instrument to predict broad bandwidth waveforms,. This can be accomplished by extracting a system efficiency factor [2] from a reference waveform, such as the echo from a planar surface, and multiplying its frequency components times the time harmonic components representing the beam and scattering amplitudes. The resulting spectrum is inverse Fourier transformed to generate a time domain RF waveform.

In order to model UT inspectability characteristics of forgings, which have entry surfaces of complex shape, it is necessary to know the appropriate geometrical parameters that define the component's surface. In the work described herein, the geometrical descriptions (coordinates of surface points, normal vectors, principal radii of curvature) of the forgings have been extracted from CAD models. Figure 1 shows an example of such a CAD model for a forged titanium alloy jet engine component. The inspectability results in this paper are computed for this forging.

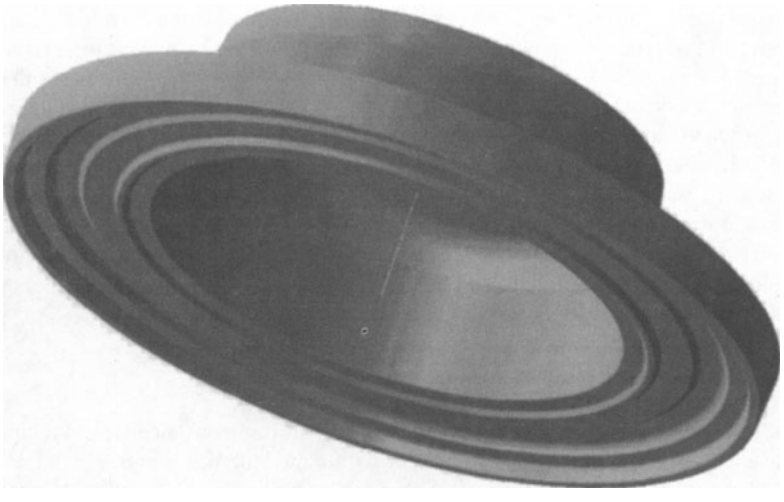

Figure 1. Solid model rendering of a titanium alloy jet engine forging.

MODEL RESULTS

The models and approach described above were used to compute ultrasonic inspection results for the titanium alloy forging shown in Fig. 1. In the simulations, the ultrasonic inspection was assumed to be performed in an immersion tank. Model inputs for the transducer, scan, material, and flaw parameters were:

Probe:
- 0.375" (0.953 cm) diameter
- 3" (7.62 cm) focal length
- 0.047" (0.12cm) beam diameter at focus
- 10 MHz center frequency
- -6dB bandwidth of 6 MHz (60%)

Scan:
- 3" (7.62 cm) water path along UT beam axis
- Normal incidence longitudinal or 45 degree shear wave modes
- 0.10" (0.254cm) coarse scan index or 0.02" (0.051cm) fine scan index
- scan is performed over both the "top" and "bottom" of the forging

Material properties:
- Water - 1 g/cc density, 0.058 in./microsec. (0.148 cm/microsec.) acoustic velocity
- Forging (titanium alloy) - 4.49 g/cc density, 0.243 in./microsec. (0.617 cm/microsec.) longitudinal wave velocity, 0.124 in./microsec. (0.315 cm/microsec.) shear wave velocity
- ultrasonic attenuation was neglected

Flaws:
- 0.016" (0.040cm) diameter flat-bottomed holes (#1 FBH) oriented perpendicular to UT beam axis
- 0.022" (0.056cm) diameter 10:1 aspect ratio (pancake-shaped) voids oriented parallel to "flow lines"

Figure 2 shows model results for an assumed coarse scan index of 0.10" (0.254cm) using normal incidence longitudinal waves. The overall outline of the figure corresponds to the portion of the profile of the forging that contains the final machined part shape, which is shown as a white outline superimposed inside the greyscale image. Greyscale intensity, as defined in the colorbar in the figure, represents the rectified signal amplitude, in volts, for #1 FBH scatterers located throughout the component and oriented normal to the ultrasonic beam. The scan is assumed to cover both the "top" and the "bottom" of the forging. At each point in the profile, the greyscale value is the maximum obtained for all transducer locations for which the ultrasonic beam strikes a flaw located at that point. The striped appearance of this inspectability map occurs because the scan index is roughly twice the focal spot size of the transducer. The scan plan used in this inspection is clearly inadequate, since the signal amplitude drops to nearly zero between successive scan index locations. In contrast, Figure 3 shows model results for an inspection that uses a 0.02" (0.051cm) scan index. Now there is little discernable drop in amplitude between successive scan lines, except near the small radius fillets at various locations around the profile. This demonstrates the utility of this modeling approach for assuring adequate scan coverage for an assumed component and UT system. Note that the measurement model employed in the simulations computes UT beam transmission into the forging based upon the surface curvature at the beam axis. This causes the apparent discontinuities in amplitude observed in Fig. 3 at transitions between linear and circular curves in the profile. Further model integration is being pursued to correctly predict the behavior at these geometrical transitions.

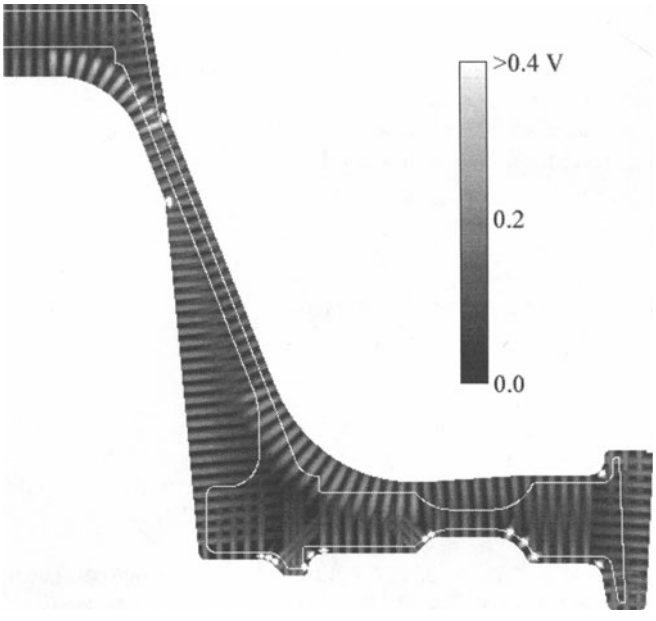

Figure 2. Model prediction of scan coverage assuming 0.10" (0.254cm) scan spacing. Signal amplitudes correspond to a #1 FBH reflector normal to the ultrasonic beam.

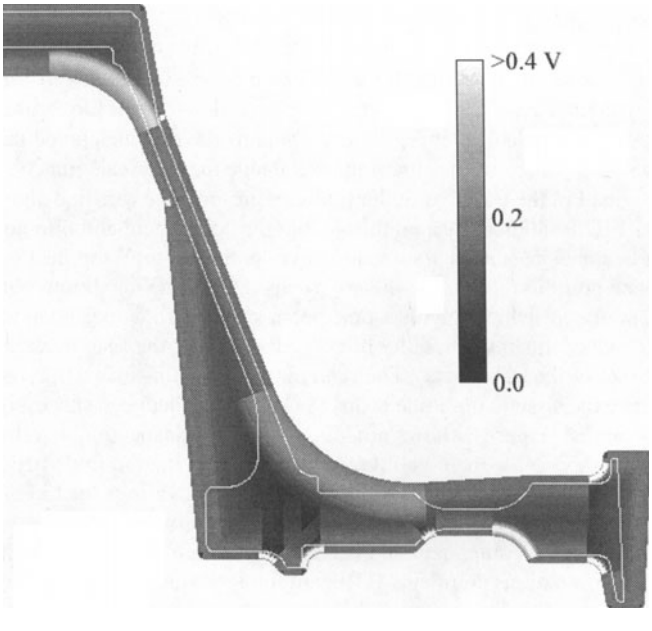

Figure 3. Model prediction of scan coverage assuming 0.02" (0.0508cm) scan spacing. Signal amplitudes correspond to a #1 FBH reflector normal to the ultrasonic beam.

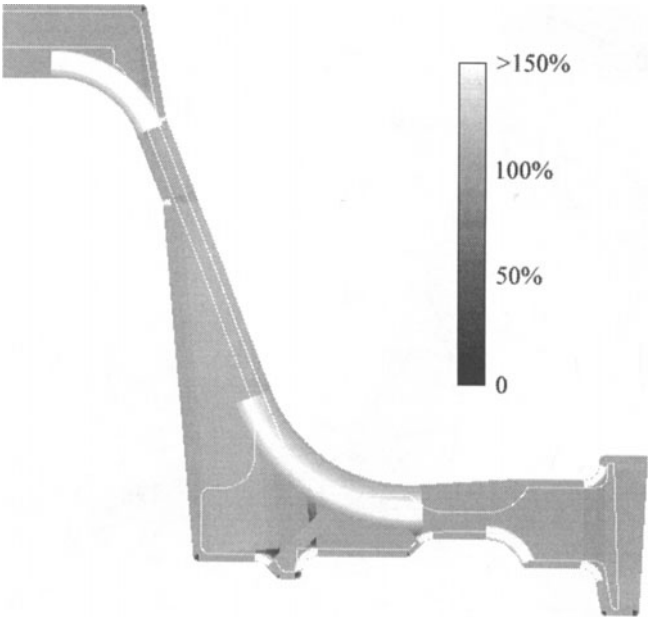

Figure 4. Model prediction of scan coverage assuming 0.01" (0.0254cm) scan spacing. Signal amplitudes are expressed relative to a distance-amplitude curve (DAC) from flat calibration blocks containing #1 FBH reflectors.

The preceding figures showed greyscale image mappings of the raw ultrasonic signal amplitudes. It is apparent in those images that the signal amplitude drops significantly as a function of depth below the surface of the forging. However, no conclusion can be drawn concerning the change in flaw detectability caused by that drop in amplitude. A common approach to address this issue is to employ distance-amplitude curve (DAC), sometimes called time variable gain (TVG), based upon a calibration measurement on standard test specimens containing FBH reflectors at several depths. As an example of this approach, the model was used to predict amplitude versus depth for #1 FBH reflectors below a flat surface. Then, the signal amplitudes for flaws at a given depth in the forging geometry were divided by the flat surface DAC value for that depth. The resulting inspectability values, expressed as a percentage of the DAC amplitude, are shown in Fig. 4. Of course, a side effect of DAC adjustments is that raising the gain of low amplitude flaw signals also raises the backscattered noise amplitude. This is a problem critical in forging inspections because the non-symmetrical beam focusing due to surface curvature distorts the beam, which can also accentuate noise levels. The modeling software does not currently predict backscattered noise levels, but models are under development in the Engine Titanium Consortium to make such predictions; see, e.g., Ref. 5.

In addition to normally incident longitudinal wave inspections, refracted angle shear wave measurements are frequently performed on forgings. The modeling software allows the transducer to be tilted relative to the component surface, and shear wave measurements are readily simulated. Figure 5 illustrates such a simulation. In this example, the transducer was assumed to be tilted 19.4 degrees clockwise in the plane of the profile, which corresponds to a 45 degree refracted shear wave in the forging.

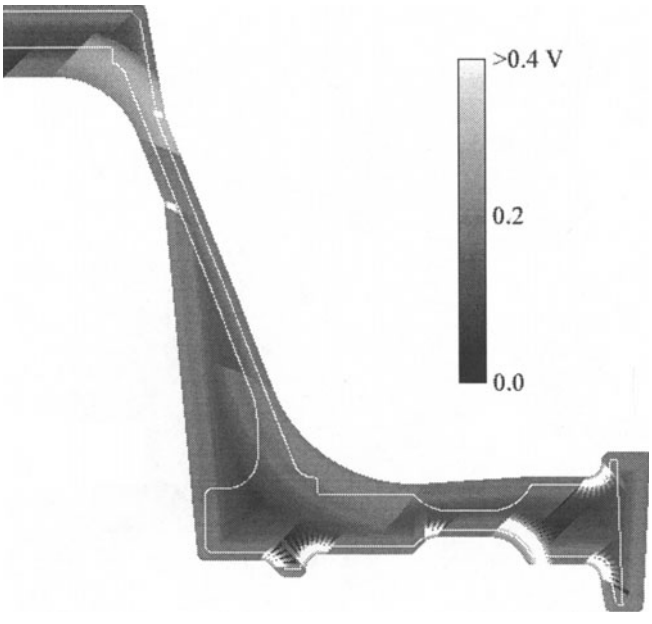

Figure 5. Model prediction of scan coverage assuming 0.02" (0.508cm) scan spacing using a 45-degree refracted shear wave. Signal amplitudes correspond to a #1 FBH reflector normal to the ultrasonic beam

One of the most common reasons for using oblique incidence inspections in forgings is to force the ultrasonic beam to propagate perpendicular forging flow lines. Figure 6 shows a portion of a photograph of an etched cross-section of a forging of the shape as that addressed in this paper. The forging process causes defects in the original billet material to be drawn-out or flattened during forging and to become aligned with the flow lines. Ultrasonic scattering from such flaws will tend to exhibit strong directional behavior. To illustrate this effect, flaws were assumed to be aligned with a set of concentric circular contours, which are shown in Figure 7. The flaws were modeled as 0.022" (0.056cm) diameter, 10:1 aspect ratio (pancake-shaped) voids. At normal incidence to the flaw, this size and shape produces the same backscattered amplitude as a #1 FBH when illuminated by the transducer defined above. Signal amplitudes for a normal incidence, longitudinal wave scan for this flaw scenario are shown in Figure 8. By comparing these results to those in Fig. 3, it is clear that the misorientation of the flaws has caused a significant drop in signal amplitude at many locations. A realistic analysis of these effects obviously requires more accurate representation of the flow line shapes. Work is underway to extract this information from commercial forging software.

SUMMARY AND SUGGESTIONS FOR FUTURE WORK

Application of models to predict ultrasonic inspectability of axially symmetric jet engine forgings provides a convenient method for specifying inspection configurations, UT system characteristics, scan plan parameters, etc. In addition, the analytical nature of the models enable parametric studies of inspection capability versus forging geometry, for example, which allows this capability to be used during the initial design of the forged

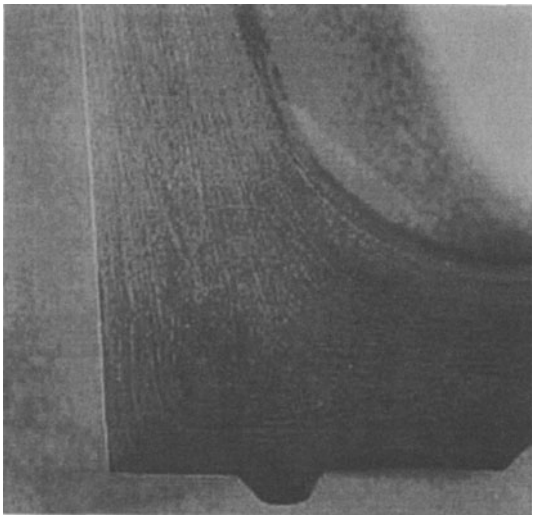

Figure 6. Photograph of a section of a forging showing material flow patterns, or "flow lines."

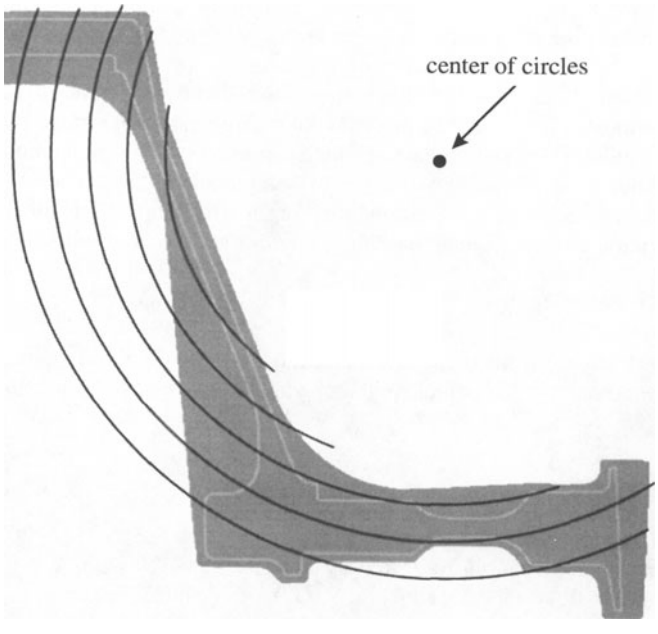

Figure 7. Schematic representation of contours for flaw orientation, intended to mimic effects on flaw orientation that would result from forging flow.

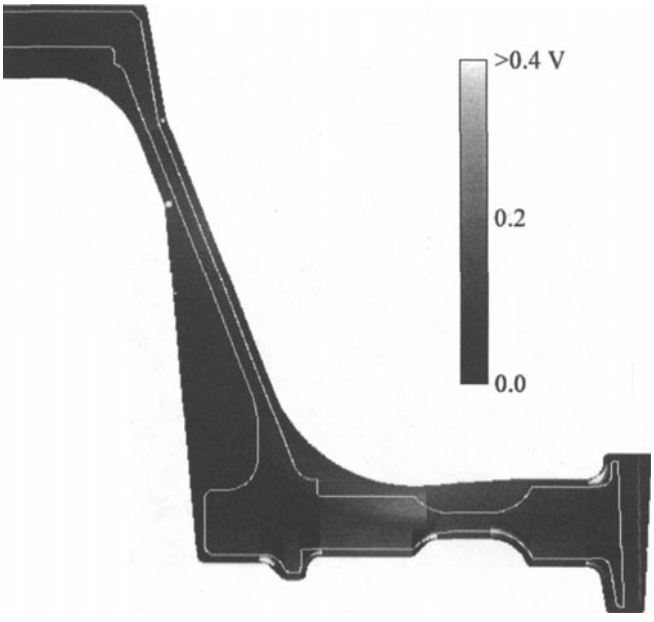

Figure 8. Signal amplitudes for pancake-shaped voids aligned with the orientation contours illustrated in Fig. 7. The void diameter was chosen to yield the same signal amplitude as a #1 FBH at normal incidence.

component. However, full use of this approach will require additional modeling and software integration. Improvements needed in the software presented here include:

- enhancements to beam model to eliminate discontinuity at geometry transitions;
- incorporation of backscattered noise due to the microstructure of the forging;
- consideration of surface roughness, which causes a drop in signal amplitude and also creates a near-surface "dead zone" which masks flaw indications;
- integration with output from commercial forging flow software to allow specification of flaw orientations and, if appropriate, material property variation.

ACKNOWLEDGMENTS

This work was performed under the sponsorship of the Engine Titanium Consortium, supported by the Federal Aviation Administration under Grant number 94G048.

REFERENCES

1. B. A. Auld, *Wave Motion 1*, 3 (1979).
2. R. B. Thompson and T. A. Gray, *J. Acoust. Soc. Am. 74*, 1279 (1983).
3. R. B. Thompson, T. A. Gray, J. H. Rose, V. G. Kogan, and E. F. Lopes, *J. Acoust. Soc. Am. 92*, 1818 (1987).
4. L. Adler and J. D. Achenbach, *J. Nond. Eval. 1*, 87 (1980).
5. F. J. Margetan, I. Yalda, R. B. Thompson, J. Umbach, U. Suh, P. J. Howard, D. C. Copley, and R. Gilmore, *Review of Progress in QNDE, vol. 16*, eds. D. O. Thompson and D. E. Chimenti., (Plenum Press, New York, 1997), p. 1555.